Laser-generated singlet oxygen is protective against beta-amyloid neurotoxicity

Olga A. Stelmashchuk[1], Viktor V. Dremin[1,2], Andrey Y. Abramov [1,3]

[1] Orel State University, Orel, 302026, Russia

[2] College of Engineering and Physical Sciences, Aston University, Birmingham, B4 7ET, UK

[3] Department of Clinical and Movement Neurosciences, UCL Queen Square Institute of Neurology, Queen Square, London, WC1N 3BG, UK

Correspondence: Prof Andrey Y. Abramov a.abramov@ucl.ac.uk

Abstract

β-Amyloid is the peptide which forms extracellular senile plaques in Alzheimer's disease. Link of the β-amyloid to inherited form of Alzheimer's disease and neurotoxicity of aggregated peptide has been suggested to the involvement of β-amyloid in the mechanism of pathology of this devastating disease. The toxicity of aggregated β-amyloid is triggered by changes in calcium signal, mitochondrial energy metabolism and oxidative stress. Laser (1267nm)-induced singlet oxygen is shown to be able to modify proteins and accelerate energy metabolism that potentially may modify the effects of β-amyloid. Using primary co-culture of neurons and astrocytes we studied the effect of laser-generated singlet oxygen on β-amyloid-induced calcium signal, mitochondrial energy metabolism and oxidative stress. We have found that singlet oxygen prevents aggregation of the full peptide βA 1-42, reduces the effect of β-amyloid on cytosolic and mitochondrial calcium elevation, reduces mitochondrial depolarization and depletion of NADH in mitochondria. As result it protected neurons and astrocytes against β-amyloid-induced cell death. Thus, singlet oxygen could play neuroprotective role.

Keywords: β-amyloid; neuron, astrocyte; singlet oxygen;

1. Introduction

Alzheimer's disease is the most common neurodegenerative disorder and the major cause of dementia. The histopathological features of this disease are extracellular senile plaques (formed by aggregated protein β-amyloid (βA)) and intracellular inclusions - nneurofibrillary tangles, which consist of aggregated tau proteins. In the monomer state, both – tau and β-amyloid play physiological roles. However, in oligomeric form full β-amyloids βA1-40 and βA1-42 become neurotoxic [1]. Mutations in the genes related to β-amyloid induce a familial form of Alzheimer's disease [2]. All these facts suggest important role of aggregated β-amyloid in the mechanism of neurodegeneration in Alzheimer's disease. β-amyloid is shown to be involved in various cellular processes which take part in the mechanism of neurodegeneration. Oligomeric and fibrillary form βA1-42 and βA1-40 are membrane-active and could form a pore in artificial and cellular membranes inducing ion conductivity [3–5]. This pore formation is dependent on the membrane cholesterol content [6] and it triggers calcium signal, mitochondrial depolarization and activation of NADPH oxidase, resulting in massive cytosolic ROS production [7]. Activation of NADPH oxidase in astrocytes is one of the key points in the mechanism of β-induced neurotoxicity, and the inhibitors of this enzyme successfully protected neurons and astrocytic cells [7,8]. Production of free radicals and excess of calcium in the matrix of mitochondria induce the opening of the mitochondrial permeability transition pore (mPTP), which causes rapid and short-term depolarization of mitochondria, accompanied by the release of cytochrome C and in some cells, activation of the DNA repairing enzyme PARP, which consumes NAD that limits NADH for mitochondria and induces mitochondrial dysfunction [9].

βA is a hydrophobic peptide that contains ROS-sensitive residues (Tyr10, His13, His14 и Met35), photo-oxidative modification of these residues by excited singlet oxygen ($^1O_2$) can alter the hydrophobicity of beta-amyloid and disrupt the self-assembly of beta-amyloid monomers [10] that may reduce the ability of βA for aggregation [11]. Singlet oxygen ($^1O_2$) is the common name for the electronically excited state of triplet oxygen, which is the lowest excited state of the oxygen dioxide molecule. Considering the ability of ROS to induce oxidative damage, the production of singlet oxygen by the illumination of photosensitizers is used to induce damage in unwanted cells and tumors [12]. It should be noted that singlet oxygen is produced in cellular enzymatic reactions by a number of peroxidase enzymes, including myeloperoxidase, lactoperoxidase, and chloroperoxidase. This occurs during reactions catalyzed by lipoxygenases and play role in physiology of cells [13].

However, there are some disadvantages and limitations to currently available photosensitive nanomaterials and after many years of study treatment with photosensitizers is still subject of discussion but not the medical treatment. Although it can be used for sterilizing effect of ROS [14] that also cannot exclude effect of the photosensitive chemicals. There are some others way to produce singlet oxygen but they are also limited by using of chemicals [15]. Relative recently, it was found that $^1O_2$ can be generated without any activating compound, by exciting cell molecules with specific wavelengths of optical radiation [16,17]. Oxygen has the highest absorption coefficient in the band 1262-1268 nm. With this in mind, lasers with a wavelength of about 1270 nm are currently widely used to generate singlet oxygen in various tissues [18]. Interestingly, the generation of singlet oxygen without the use of photosensitizers has been shown to exhibit non-damaging effects such as activation of bioenergetics in brain cells and lack of effect on opening of mitochondrial mPTP [19,20].

Here, we show that 1267 nm laser-induced singlet oxygen protects neurons and astrocytes against βA-induced cell death. Singlet oxygen changes the ability of full peptide βA 1-42 for aggregation and significantly reduces β-amyloid-triggered calcium signal in cytosol and mitochondria. Importantly, the generation of singlet oxygen protects neurons and astrocytes against βA-induced PARP activation and NADH depletion which has always been linked to ROS production and ultimately, to oxidative stress.

2. Methods

Cell culture

Co-cultures of cortical neurons and glial cells were prepared as described previously with modifications [21], from Wistar rat pups 2–4 days post-partum. Cortices were washed into ice-cold PBS (Ca^{2+}, Mg^{2+}-free, Gibco, UK), minced and trypsinised (0.25% for 15 min at 37° C), triturated and plated on poly-D-lysine-coated coverslips and cultured in Neurobasal A medium (Gibco, USA) supplemented with B-27 (Invitrogen, UK) and 2 mM L-glutamine. Cultures were maintained at 37˚C in a humidified atmosphere of 5% CO_2 and 95% air and used after 12 days.

Laser specification

For this study, a laser diode LD-1267-PM 500 (Innolume GmbH, Germany) for laser radiation at a wavelength of 1267 nm, and a specially manufactured quartz fiber-optic cable were used. The cable provided radiation transmission with minimal signal attenuation in the spectral range of 400-2000 nm and a numeric aperture of 0.22. The results of the *in silico* study of the distribution of the thermal field in biological tissue and additional thermal imaging measurements [22] helped to select safe laser irradiation parameters to avoid overheating of the cell culture and produced a singlet oxygen [23].

Singlet oxygen production

The production of singlet oxygen was quantified using 10 μM Singlet Oxygen Sensor Green (SOSG, Invitrogen, Oregon, USA), with excitation at 488 nm and emission at 525 nm. Data acquisition was carried out in real-time to capture dynamic changes in singlet oxygen levels.

Measurement of cytosolic Ca^{2+} and mitochondrial membrane potential

Simultaneous measurements of intracellular Ca^{2+} and mitochondrial membrane potential were produced after loading with 5 μM Fura-2 AM and Rhodamine 123 (Invitrogen by Thermo Fisher Scientific, USA) in HBSS, using excitation at 340, 380 and 490 nm and emission at 515 (Cairn Research, Kent, UK).

Measurement of cytosolic and mitochondrial Ca^{2+}

For measurement of cytosolic and mitochondrial Ca^{2+} concentrations, 30 min incubation of the neurons and astrocytes with 5 μM Fluo-4 AM or 5 μM X-Rhod-1 AM at room temperature was used for loading. Fluorescence of fluo-4 and x-rhod-1 was measured using a Zeiss 900 confocal microscope (40X objective) using 488 nm and 563 nm lasers for excitation and emission at 505-550 nm or 580-630 nm, respectively. All data presented were obtained on at least 5 coverslips and 2-3 different cell preparations.

ROS (superoxide production) measurements

Reactive oxygen species (mainly superoxide production) was measured using 5 μM dihydroethidium (DHE, Invitrogen Oregon, USA) as a ratio of oxidized product excitation 530nm and emission above 560nm and non-oxidized (DHE) excitation 380 nm with emission at 450 nm. No loading of cells was used and measurements were

taken after application of 5 μM DHE and this probe was in the medium during the time of experiment.

Measurement of the NADH

Mitochondrial NADH autofluorescence was measured using excitation light from a monochromator at 360 nm. The emitted light was reflected through a 455 nm long-pass filter to a cooled CCD camera. To separate mitochondrial NADH autofluorescence from cytosolic NADH signal and NADPH autofluorescence activation, the fluorescence was taken between minimal values after activation of respiration with 1μM FCCP and maximal NADH after inhibition of mitochondrial respiration and NADH consumption with 1 mM KCN [21].

Thioflavin T fluorescence spectroscopy

The ability of singlet oxygen to inhibit β-amyloid aggregation (βA25-35 and βA1-42) was evaluated using 25μM thioflavin T (ThT). ThT become fluorescent when bound to amyloid aggregates and used as an indicator of peptide aggregation with excitation by 450 nm and measured at 482 nm. Fluorescence measurements were performed on a FLUOstar Omega multifunctional microplate reader using 90-well microplates.

Fluorescence measurements were taken immediately after mixing of the βA/ThT mixtures and continues for 5 hours. The relative changes in fluorescence intensity of ThT were calculated as $(F-F_0)/F_0$, where F and F_0 are the fluorescence intensities of ThT in the presence and absence of βA peptides, respectively.

Cell death

For toxicity assays, the cells were loaded simultaneously with 20 μM propidium iodide (PI), which exhibits a red fluorescence following a loss of membrane integrity and binding to the nuclea, and 4.5 μM Hoechst 33342, which labels nuclei blue, to count the total number of cells.

Data analysis and statistics

Data and statistical analyses were performed using OriginPro (OriginLab Corp., Northampton, USA) software. Data are presented as means ± standard error of the mean (SEM). Differences were considered to be significantly different if $p<0.05$ by ANOVA with the Tukey post-hoc test.

3. Results

Singlet oxygen changes βA-induced calcium signal and mitochondrial depolarization

β-amyloid is able to induce calcium signal through the formation of a pore on the membrane and mitochondrial depolarization in astrocytes and to induce cell death in neurons [4,7,24].

In agreement with previously published literature [4,7,25], simultaneous measurement of $[Ca^{2+}]_c$ with Fura-2 and mitochondrial membrane potential (Δψm) with potential-sensitive probe Rhodamine-123 showed that the application of the full peptide βA 1-42 (5 μM) or the short peptide βA 25-35 (5 μM) to primary cultures induced an increase in $[Ca^{2+}]_c$ in astrocytes (n=290 cells), but not in neurons from the same co-culture (Fig. 1 A,B,C,G). Importantly, application of the βA1-42 or βA 25-25 also induced mitochondrial depolarization (Fig 1A, B, D, H). The generation of the singlet oxygen by the illumination of the cells with a 1267 nm laser (100 J/cm^2) following the application of beta-amyloid led to a reduction in the amplitude of the βA-induced calcium signal for βA 25-35 (n=120 astrocytes) to 44±5% of control (n = 120 astrocytes; $p<0.001$) and (βA 1-42, n=89 astrocytes) to 57±5% of control (n=109; $p<0.01$; Fig. 1 C,G). Laser-induced singlet oxygen production decreased the effect of βA 1–42 on Δψm to 59±5% (n = 109; $p<0.01$; Fig. 1 D,H) and for βA 25–35 to 79±6% of control (n=120 astrocytes) in astrocytes (Fig. 1 E,F). Thus, singlet oxygen decreases effects of βA on $[Ca^{2+}]_c$ and mitochondrial membrane potential.

Singlet oxygen prevents mitochondrial Ca^{2+} overload induced by βA

β-amyloid-induced mitochondrial depolarization is partially dependent on mitochondrial calcium uptake [25,26]. In order to investigate if laser-produced singlet oxygen has an effect on β-amyloid-induced mitochondrial calcium uptake, we measured $[Ca^{2+}]_m$ with fluorescent indicator X-Rhod-1 and cytosolic Ca^{2+} with a Fluo-4. In agreement with experiments with Fura-2 measurements (Fig. 1), the application of 5 μm βA1-42 or 5 μm βA25-35 to a co-culture of cortical neurons and astrocytes trigger of changes in $[Ca^{2+}]_c$ of astrocytes (n=77 astrocytes for βA1-42; n = 105 astrocytes for βA25-35; Fig. 2 A,B). It should be noted that both peptides – βA1-42 and βA 25-35 induced calcium signal in the cytosol, which triggered the mitochondrial calcium uptake (Fig. 2A,B). However,

treatment of the cells with laser-induced singlet oxygen in the presence of βA significantly reduced the amplitude the $[Ca^{2+}]_c$ changes for βA 25-35 to 15±3% of control (n=111 astrocytes; p<0.001; Fig. 2 C) and for βA1-42 to 63±3% of control (n=88; p<0.01; Fig. 2G) and reduced the amplitude of mitochondrial calcium uptake. Hence, for βA 25-35 it decreased to 39±6% of control (n=111 astrocytes; p < 0.001; Fig. 2D) and for βA1-42 to 36±4% of control (n=88; p<0.001; Fig. 2H). Thus, singlet oxygen decreases βA-induced mitochondrial calcium uptake in astrocytes.

Singlet oxygen prevents βA-induced depletion of mitochondrial NADH

βA-induced calcium signal activates NADPH oxidase, resulting in oxidative stress and mitochondrial depolarization which is induced by calcium and depletion of mitochondrial substrate NADH by the DNA repairing enzyme poly(ADP-ribose)-polymerase (PARP) [7,9]. In agreement with previously published results, the application of βA 25-35 (5 μM; n=120 cells) or βA1-42 (5 μM; n=89 cells) induced slow and progressive decrease of NADH autofluorescence of cortical co-culture compared to control (Fig. 3 A,B,C). Preincubation of primary co-cultures with the inhibitors of PARP, 3-aminobenzamide (3AB, 1 mM, 20 min), reduced the effect of β-amyloid on the NADH autofluorescence signal (Fig. 3 D,E).

It should be noted that the generation of singlet oxygen by 1267 nm laser not only prevents βA-induced depletion of mitochondrial NADH pool but even increases it from 30±2% (βA 25-35, n =112 cells) to 143.7 ± 4.3% (n = 110 cells; p < 0.001) and from 59± 5% (βA 1-42, n =112 cells) to 154 ± 6 (n=112 cells; p < 0.001) relative to control (n = 150 cells) (Fig. 3 F,G,H). Thus, singlet oxygen inhibits NADH depletion, which is induced by another ROS – superoxide anion which is produced in the NADPH oxidase in response to the action of βA [27].

1267 nm laser produce singlet oxygen production but decrease βA-induced superoxide production

In agreement with the previously published [19,20] illumination of the primary neurons and astrocytes with 1267 nm laser (100 J/cm^2) induced an increase in the rate of SOSG fluorescence that corresponds to an increase of singlet oxygen production (Fig. 4A). Interestingly, Application of βA1-42 (1μM) did not change the rate of SOSG oxidation (Fig. 4B). In contrast, application of βA1-42 or βA 25-35 induced activation of ROS production measured with dihydroethidium (mainly superoxide anion; Fig. 4C,E).

Importantly, 1267 nm induced singlet oxygen production, significantly reducing the effect of βA1-42 on ROS production (Fig. 4D,E).

In order to test whether laser-induced singlet oxygen and βA-induced superoxide anion quench the effect of each other on oxidative stress in neurons and astrocytes, we measured the effect of these triggers on the level of the endogenous antioxidant GSH using the fluorescent probe monochlorobimane (MCB, 50 μM). Application of βA 25-35 expectably decreases the level of GSH to 73±2% of control (n=400 cells; $p<0.01$; Fig. 4F,G) while the 1267 nm laser (100 J/cm^2) decreased it even more – to 50±3% of control (n=420 cells; Fig. 4F,G). However, combination of the treatment of cells with laser irradiation and βA 25-35 kept the level of GSH similar to laser only (Fig. 4F,G). Thus, laser-induced singlet oxygen does not protect neurons and astrocytes against βA-induced oxidative stress.

Singlet oxygen alters aggregation of βA 1-42

Activity and toxicity of βA are dependent on oligomerization [5]. The ability of βA to be aggregated was assessed by a fluorescent probe Thioflavin T (ThT, 25 μM). ThT bound to amyloid aggregates and fluorescence and can, therefore, be used as an indicator of peptide aggregation. Pretreatment of βA with 1267nm laser significantly reduced the ThT fluorescence in experiments with full-length peptide βA 1-42 (5μM) - from 206±30% (n=24 experiments) to 132±10% of control (n=24 experiments, $p<0.001$) (Fig. 5 A,B). It should be noted that the short length peptide βA 25-35 did not induce aggregation, and treatment of these peptides with a 1267 nm laser did not change ThT fluorescence in these experiments.

Singlet oxygen protects neurons and astrocytes against Aβ-induced neurotoxicity

To investigate if laser-generated singlet oxygen can modify the toxicity of βA, propidium iodide, which indicates cells with permeable plasma membrane (necrosis), and Hoechst 33342 for detection of all cells were used. Incubation (24 hours) of co-cultures of neurons and astrocytes with full-length peptide β1-42 or short-length peptide βA25-35 induced a relatively high,3-fold increase in the number of dead cells compared to the control of laser 1267 nm-treated cells (Fig. 6A-B). Laser-induced singlet oxygen protected neurons and astrocytes against βA-induced toxicity. Thus, percentage of dead cells decreased from 60 ± 3% (βA 25-35, n=450 cells) to 38 ± 4% (n=470 cells;

p<0.001) and from 57±2% (βA 1-42, n=320 cells) to 36±2% of control (n=440 cells; p<0.001) (Fig. 6A-B). It should be noted that laser irradiation alone did not increase the number of dead cells compared to the control (Fig. 6A).

4. Discussion

Here we show that laser-generated singlet oxygen protects neurons and astrocytes against β-amyloid neurotoxicity. βA is known to be able to increase ROS production (mainly superoxide and hydrogen peroxide through the NADPH oxidase) and to induce oxidative stress and mitochondrial dysfunction due to the activation of PARP and limitation in substrates [7,9,28]. Activation of ROS production in neurons and astrocytes with photosensitizers (that should also produce singlet oxygen) induced similar activation of PARP and substrate-limiting inhibition of mitochondrial respiration [29,30]. We can suggest that a combination of superoxide from NADPH oxidase and laser-generated singlet oxygen could enhance each other's action. However, treatment of co-culture of neurons and astrocytes with 1267 nm laser reduced the effect of βA on Δψm (Fig. 1). Singlet oxygen decreases the level of GSH but this effect is similar to results that both – βA and laser 1267 nm irradiation used for cell treatment (Fig. 4). It suggests that singlet oxygen prevents βA-induced ROS production and some other effects.

In our experiments, laser-induced singlet oxygen inhibited the aggregation of βA 1-42 and had no effect on the short length peptide βA25-35, which did not induce aggregation (Fig. 5). Our results are in agreement with a number of publications which indicate scavenging the βA plaques [31] and reduction of βA aggregates by photo-oxidation [11,32]. However, using photosensitizers can induce activation of other forms of ROS and can be very toxic for brain cells. Using the 1267 nm for the generation of singlet oxygen we have found that in these doses it is not toxic for neurons (Fig. 6) and even activates the mitochondrial energy metabolism in neurons and astrocytes [19]. Singlet oxygen did not change the aggregation of βA25-35 but significantly reduced the toxicity of this peptide and its effect on the Δψm, cytosolic and mitochondrial calcium signal. This may suggest that singlet oxygen oxidizes βA25-35 and changes its activity without an effect on aggregation or using some other ways for protection.

One of the possible, or additional, ways for neuroprotection could be an effect of singlet oxygen on mitochondrial respiration and Δψm. Laser-generated singlet oxygen can increase the mitochondrial pool of NADH [19], and in our experiments, singlet oxygen not only prevents βA-induced depletion of NADH in mitochondria but also increases it (Fig. 3).

One of the first stages in βA-toxicity is the activation of the calcium signal in astrocytes [8]. βA induces a calcium signal in astrocytes and, in the later stages, also in neurons through the incorporation of aggregated peptides into the membrane, for which short-length peptide aggregation is not essential [4]. Importantly, treatment of the cells with 1267 nm laser significantly reduced βA-induced calcium signal in cytosol and mitochondria, suggesting that deactivation of the βA 1-42 (through inhibition of aggregation) and βA 25-35 (possibly through oxidation) is the main suppressor of toxicity of this peptide.

Another possible explanation of the protective role of singlet oxygen, which can explain the effect on βA 25-35, may be activation of antioxidant pathways such as Nrf2 or Hsp70, which also can play a role as a chaperone [33,34].

Thus, 1267 nm laser-generated singlet oxygen is not toxic in the studied doses and can be potentially used as a cell protective strategy in Alzheimer's disease.

Acknowledgements

The work was supported by the Mega Grant 075-15-2025-011 (Russian Federation)

Conflict of Interest:

The authors have no conflicts of interest to declare.

Availability of Data and Materials:

The data that support the findings of this study are available from the corresponding author, upon reasonable request.

Author Contributions

Experiments – OAS. Conceptualization and design of experiments – AYA, VVD, OAS. Analysis – OAS, VVD. Writing OAS, AYA. Corrections – AYA, OAS, VVD. All authors read and approved the final manuscript.

References

[1] M.B. Podlisny, D.M. Walsh, P. Amarante, B.L. Ostaszewski, E.R. Stimson, J.E. Maggio, D.B. Teplow, D.J. Selkoe, Oligomerization of endogenous and synthetic amyloid β-protein at nanomolar levels in cell culture and stabilization of monomer by Congo red, Biochemistry. 37 (1998) 3602–3611.

[2] D.J. Selkoe, J. Hardy, The amyloid hypothesis of Alzheimer's disease at 25 years, EMBO Mol. Med. 8 (2016) 595–608.

[3] N. Arispe, H.B. Pollard, E. Rojas, Giant multilevel cation channels formed by Alzheimer disease amyloid beta-protein [A beta P-(1-40)] in bilayer membranes., Proc. Natl. Acad. Sci. 90 (1993) 10573–10577.

[4] A.Y. Abramov, L. Canevari, M.R. Duchen, Changes in intracellular calcium and glutathione in astrocytes as the primary mechanism of amyloid neurotoxicity, J. Neurosci. 23 (2003) 5088–5095.

[5] P. Narayan, K.M. Holmström, D.-H. Kim, D.J. Whitcomb, M.R. Wilson, P. St. George-Hyslop, N.W. Wood, C.M. Dobson, K. Cho, A.Y. Abramov, Rare individual amyloid-β oligomers act on astrocytes to initiate neuronal damage, Biochemistry. 53 (2014) 2442–2453.

[6] A.Y. Abramov, M. Ionov, E. Pavlov, M.R. Duchen, Membrane cholesterol content plays a key role in the neurotoxicity of β-amyloid: implications for Alzheimer's disease, Aging Cell. 10 (2011) 595–603.

[7] A.Y. Abramov, L. Canevari, M.R. Duchen, β-Amyloid Peptides Induce Mitochondrial Dysfunction and Oxidative Stress in Astrocytes and Death of Neurons through Activation of NADPH Oxidase, J. Neurosci. (2004).

[8] P.R. Angelova, A.Y. Abramov, Interaction of neurons and astrocytes underlies the mechanism of Aβ-induced neurotoxicity, Biochem. Soc. Trans. 42 (2014) 1286–1290.

[9] R. Abeti, A.Y. Abramov, M.R. Duchen, β-amyloid activates PARP causing astrocytic metabolic failure and neuronal death, Brain. (2011).

[10] J. Yang, W. Chi, W.-J. Shi, L. Zhang, J.-W. Yan, An in situ-triggered and chemi-excited photooxygenation system for Aβ aggregates, Chem. Eng. J. 456 (2023) 140998.

[11] P. Bondia, J. Torra, C.M. Tone, T. Sawazaki, A. Del Valle, B. Sot, S. Nonell, M. Kanai, Y. Sohma, C. Flors, Nanoscale view of amyloid photodynamic damage, J. Am. Chem. Soc. 142 (2019) 922–930.

[12] T. Soleymani, M. Abrouk, K.M. Kelly, An analysis of laser therapy for the treatment of nonmelanoma skin cancer, Dermatologic Surg. (2017).

[13] J.R. Kanofsky, Singlet oxygen production by lactoperoxidase: halide dependence and quantitation of yield, J. Photochem. 25 (1984) 105–113.

[14] Y. Wang M. Li, W. Liu, L. Jiang, Illuminating the future of food microbial control: From optical tools to Optogenetic tools, Food Chem. 471 (2025) 142474.

[15] M.R. Krishnendu, D. Mehta, S. Singh, CeO_2- and Mn_3O_4-based nanozymes exhibit scavenging of singlet oxygen species and hydroxyl radicals, Nanoscale (2025).

[16] A. Blazquez-Castro, Direct $^1O_2$ optical excitation: A tool for redox biology, Redox Biol. 13 (2017) 39–59.

[17] V. Dremin, O. Semyachkina-Glushkovskaya, E. Rafailov, Direct laser-induced singlet oxygen in biological systems: application from in vitro to in vivo, IEEE J. Sel. Top. Quantum Electron. 29 (2023) 1–11.

[18] S.G. Sokolovski, S.A. Zolotovskaya, A. Goltsov, C. Pourreyron, A.P. South, E.U. Rafailov, Infrared laser pulse triggers increased singlet oxygen production in tumour cells, Sci. Rep. 3 (2013) 1–7.

[19] S.G. Sokolovski, E.U. Rafailov, A.Y. Abramov, P.R. Angelova, Singlet oxygen stimulates mitochondrial bioenergetics in brain cells, Free Radic. Biol. Med. 163 (2021) 306–313.

[20] I.N. Novikova, E. V Potapova, V. V Dremin, A. V Dunaev, A.Y. Abramov, Laser-induced singlet oxygen selectively triggers oscillatory mitochondrial permeability

transition and apoptosis in melanoma cell lines, Life Sci. 304 (2022) 120720.

[21] X. Chen, A.Y. Vinokurov, E.A. Zherebtsov, O.A. Stelmashchuk, P.R. Angelova, N. Esteras, A.Y. Abramov, Variability of mitochondrial energy balance across brain regions, J. Neurochem. (2020).

[22] V. Dremin, I. Novikova, E. Rafailov, Simulation of thermal field distribution in biological tissue and cell culture media irradiated with infrared wavelengths, Opt. Express. 30 (2022) 23078–23089.

[23] I. Makovik, A. Vinokurov, A. Dunaev, E. Rafailov, V. Dremin, Efficiency of direct photoinduced generation of singlet oxygen at different wavelengths, power density and exposure time of laser irradiation, Analyst. 148 (2023) 3559–3564.

[24] N. Arispe, E. Rojas, H.B. Pollard, Alzheimer disease amyloid beta protein forms calcium channels in bilayer membranes: blockade by tromethamine and aluminum., Proc. Natl. Acad. Sci. 90 (1993) 567–571.

[25] E.F. Shevtsova, P.R. Angelova, O.A. Stelmashchuk, N. Esteras, N.A. Vasil'eva, A. V Maltsev, P.N. Shevtsov, A. V Shaposhnikov, V.P. Fisenko, S.O. Bachurin, Pharmacological sequestration of mitochondrial calcium uptake protects against dementia and β-amyloid neurotoxicity, Sci. Rep. 12 (2022) 1–17.

[26] R. Abeti, A.Y. Abramov, Mitochondrial Ca^{2+} in neurodegenerative disorders, Pharmacol. Res. 99 (2015) 377–381.

[27] R. Abeti, A.Y. Abramov, M.R. Duchen, β-amyloid activates PARP causing astrocytic metabolic failure and neuronal death, Brain. 134 (2011) 1658–1672.

[28] S. Gandhi, A.Y. Abramov, Mechanism of oxidative stress in neurodegeneration, Oxid. Med. Cell. Longev. 2012 (2012) 428010.

[29] E. Berezhnaya, M. Neginskaya, A.B. Uzdensky, A.Y. Abramov, Photo-induced oxidative stress impairs mitochondrial metabolism in neurons and astrocytes, Mol. Neurobiol. 55 (2018) 90–95.

[30] J.-C. Ahn, J.-W. Kang, J.-I. Shin, P.-S. Chung, Combination treatment with photodynamic therapy and curcumin induces mitochondria-dependent apoptosis in AMC-HN3 cells, Int. J. Oncol. 41 (2012) 2184–2190.

[31] X. Shao, M. Li, C. Yan, C. Wang, X. Wang, P. Guan, X. Hu, L. Fan,

Photocatalytic, photothermal, and blood-brain barrier-permeable carbon nanodots: A potent multifunctional scavenger for β-amyloid plaque, Colloids Surfaces B Biointerfaces. 246 (2025) 114380.

[32] A. Taniguchi, Y. Shimizu, K. Oisaki, Y. Sohma, M. Kanai, Switchable photooxygenation catalysts that sense higher-order amyloid structures, Nat. Chem. 8 (2016) 974–982.

[33] A.T. Dinkova-Kostova, L. Baird; K.M. Holmström, C.J. Meyer, A.Y. Abramov, The spatiotemporal regulation of the Keap1–Nrf2 pathway and its importance in cellular bioenergetics, Biochem. Soc. Trans. 43 (2015) 602–610.

[34] A.Y. Vinokurov, A.A. Palalov, K.A. Kritskaya, S.V. Demyanenko, D.G. Garbuz, M.B. Evgen'ev, N.Esteras, A.Y. Abramov, Cell-permeable HSP70 protects neurons and astrocytes against cell death in the rotenone-induced and familial models of Parkinson's disease, Mol. Neurobiol. 61 (2024) 7785–7795.

Figure Legends

Figure 1. Effects of 1267 nm laser-produced singlet oxygen on βA-induced calcium signal and mitochondrial depolarisation. Simultaneous measurements of Fura-2 ratio and Rh123 fluorescence in cells treated with 5 μM βA 25-35 (A) or 5μM βA 1-42 (B). FCCP (1μM) is applied to depolarize Δψm and calibrate Rh123 signal. (C, D) Quantification of βA-induced Ca^{2+} signal (C) and mitochondrial membrane potential (D) in βA 25-35-treated cells, with and without 1267 nm laser exposure. (E, F) Changes in Fura-2 ratio and Rh123 fluorescence upon 1267nm laser irradiation (orange bar) in βA 25-35 (E) and βA 1-42 (F)-treated cells. (G, H) Quantification of βA-induced Ca^{2+} signal (G) and mitochondrial membrane potential (H) in βA 1-42-treated cells after 1267 nm laser treatment.

Figure 2. Effects of 1267 nm laser-produced singlet oxygen on βA-induced cytosolic and mitochondrial calcium signal in primary astrocytes from co-culture with neurons. (A, B) Changes in Fluo-4 fluorescence (cytosolic Ca^{2+} indicator) and X-rhod-1 fluorescence (mitochondrial Ca^{2+} indicator) in cells treated with βA 25-35 (A) and βA 1-42 (B). FCCP (red bar) was used to uncouple mitochondria. (C, D) Quantification of mitochondrial Ca^{2+} signal in βA 25-35-treated cells with and without laser exposure ($p<0.001$). (E, F) Changes in Fluo-4 and X-rhod-1 fluorescence upon laser irradiation (orange bar) in βA 25-35 and βA 1-42-treated cells. (G, H) Quantification of mitochondrial Ca^{2+} levels in βA 1-42-treated cells after laser treatment.

Figure 3. 1267 nm laser-generated singlet oxygen protects mitochondrial NADH in astrocytes against β-amyloid-induced depletion. (A) Representative trace of NADH autofluorescence in control neurons and astrocytes with sequential addition of 1μM FCCP (mitochondrial uncoupler which induce consumption of mitochondrial NADH) and KCN (complex IV inhibitor which blocks respiration and consumption of NADH in mitochondria) to determine the total NADH pool. (B, C) Changes in NADH autofluorescence in cells treated with 5 μM βA 25-35 (B) and 1 μM βA 1-42 (C). (D, E) Effects of 1 mM 3AB (PARP inhibitor) on NADH levels in βA-treated cells, indicating that PARP activation contributes to NADH depletion. (F, G) Changes in NADH autofluorescence upon laser irradiation (orange bar) in βA 25-35 (F) and βA 1-42 (G)-treated neurons and astrocytes. (H) Quantification of NADH levels across experimental groups, demonstrating significant restoration by laser treatment. **p<0.01; ***p<0.001).

Figure 4. Effect of 1267 nm laser on generation of singlet oxygen, βA-induced ROS production and GSH levels in neurons and astrocytes. (A) Effect of 1267nm laser on singlet oxygen production in neurons and astrocytes. B- effect of 5 μM βA1-42 on singlet oxygen production in neurons and astrocytes. C, D, E – effect of 5 μM βA1-42 on the rate of ROS production with or without laser 1267nm treatment. F- Measurements of monochlorobimane (MCB) fluorescence, an indicator of intracellular glutathione levels. The data presented as % of untreated control. G- Representative images of MCB fluorescence in astrocytes and neurons under different conditions: control, 1267nm laser, 5μM βA 25-35, laser + 5μM βA 25-35. βA 25-35 reduces fluorescence intensity, while laser treatment preserves intracellular glutathione levels. **p<0.01; ***p<0.001

Figure 5. Effects of 1267 nm laser irradiation on β-amyloid aggregation. (A) Thioflavin T (ThT) fluorescence kinetics showing amyloid fibril formation over time for βA 25-35 and βA 1-42 with and without laser treatment. Higher ThT fluorescence indicates increased fibrillization. (B) Quantification of ThT fluorescence intensity expressed as a percentage of control. βA 1-42 exhibits significantly higher fibrillization ($p < 0.001$), while laser treatment reduces fibril formation for βA 1-42 ($p<0.001$).

Figure 6. 1267 nm laser generated singlet oxygen protect neurons and astrocytes against β-amyloid-induced cell death. (A) Quantification of dead cells (%) under different conditions. 24-hour incubation of cells with 5μM βA 25-35 and 5μM βA 1-42 significantly increases the number of dead cells compared to control ($p<0.001$), while laser treatment reduces β-amyloid-induced toxicity ($p < 0.001$). (B) Representative images of Hoechst 33342 (blue; live) and PI (red; dead cells) fluorescence.

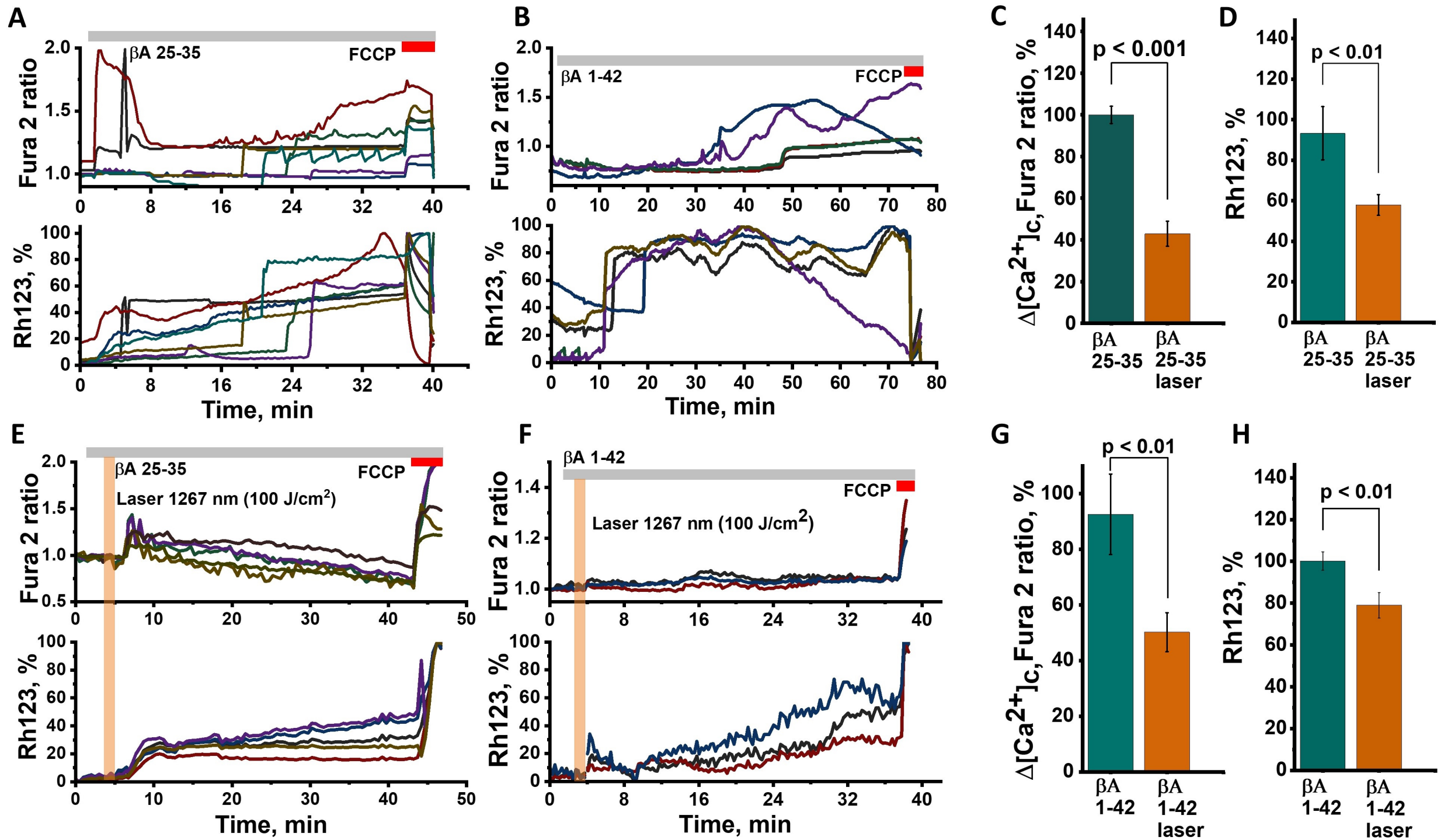
A
βA 25-35
FCCP
Fura 2 ratio
Rh123, %
Time, min
B
βA 1-42
FCCP
Fura 2 ratio
Rh123, %
Time, min
C
p < 0.001
Δ[Ca2+]c, Fura 2 ratio, %
βA 25-35
βA 25-35 laser
D
p < 0.01
Rh123, %
βA 25-35
βA 25-35 laser
E
βA 25-35
FCCP
Laser 1267 nm (100 J/cm2)
Fura 2 ratio
Rh123, %
Time, min
F
βA 1-42
FCCP
Laser 1267 nm (100 J/cm2)
Fura 2 ratio
Rh123, %
Time, min
G
p < 0.01
Δ[Ca2+]c, Fura 2 ratio, %
βA 1-42
βA 1-42 laser
H
p < 0.01
Rh123, %
βA 1-42
βA 1-42 laser

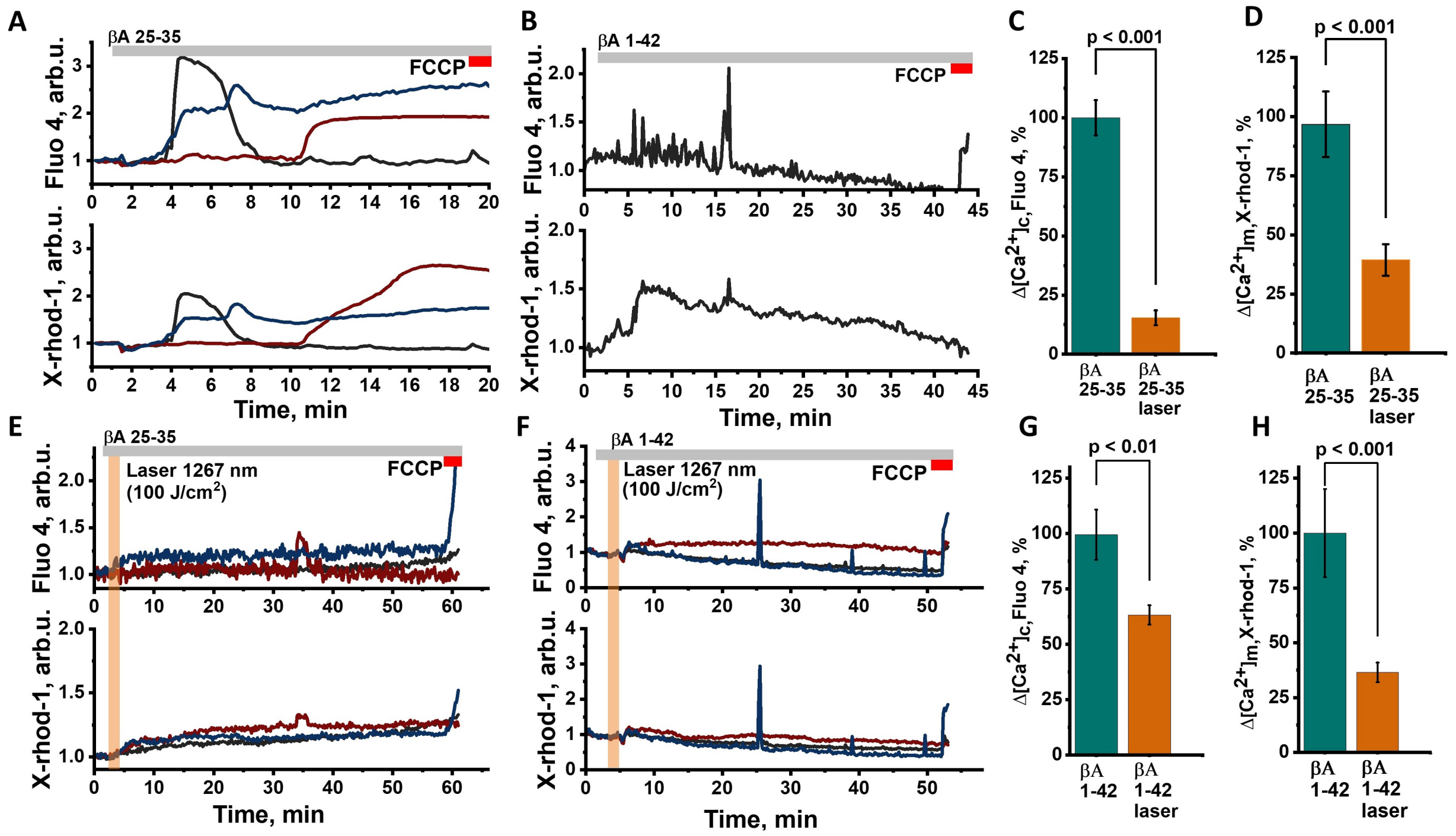
A
βA 25-35
FCCP
Fluo 4, arb.u.
X-rhod-1, arb.u.
Time, min
B
βA 1-42
FCCP
Fluo 4, arb.u.
X-rhod-1, arb.u.
Time, min
C
p < 0.001
Δ[Ca2+]c,Fluo 4, %
βA 25-35
βA 25-35 laser
D
p < 0.001
Δ[Ca2+]m,X-rhod-1, %
βA 25-35
βA 25-35 laser
E
βA 25-35
Laser 1267 nm (100 J/cm2)
FCCP
Fluo 4, arb.u.
X-rhod-1, arb.u.
Time, min
F
βA 1-42
Laser 1267 nm (100 J/cm2)
FCCP
Fluo 4, arb.u.
X-rhod-1, arb.u.
Time, min
G
p < 0.01
Δ[Ca2+]c,Fluo 4, %
βA 1-42
βA 1-42 laser
H
p < 0.001
Δ[Ca2+]m,X-rhod-1, %
βA 1-42
βA 1-42 laser

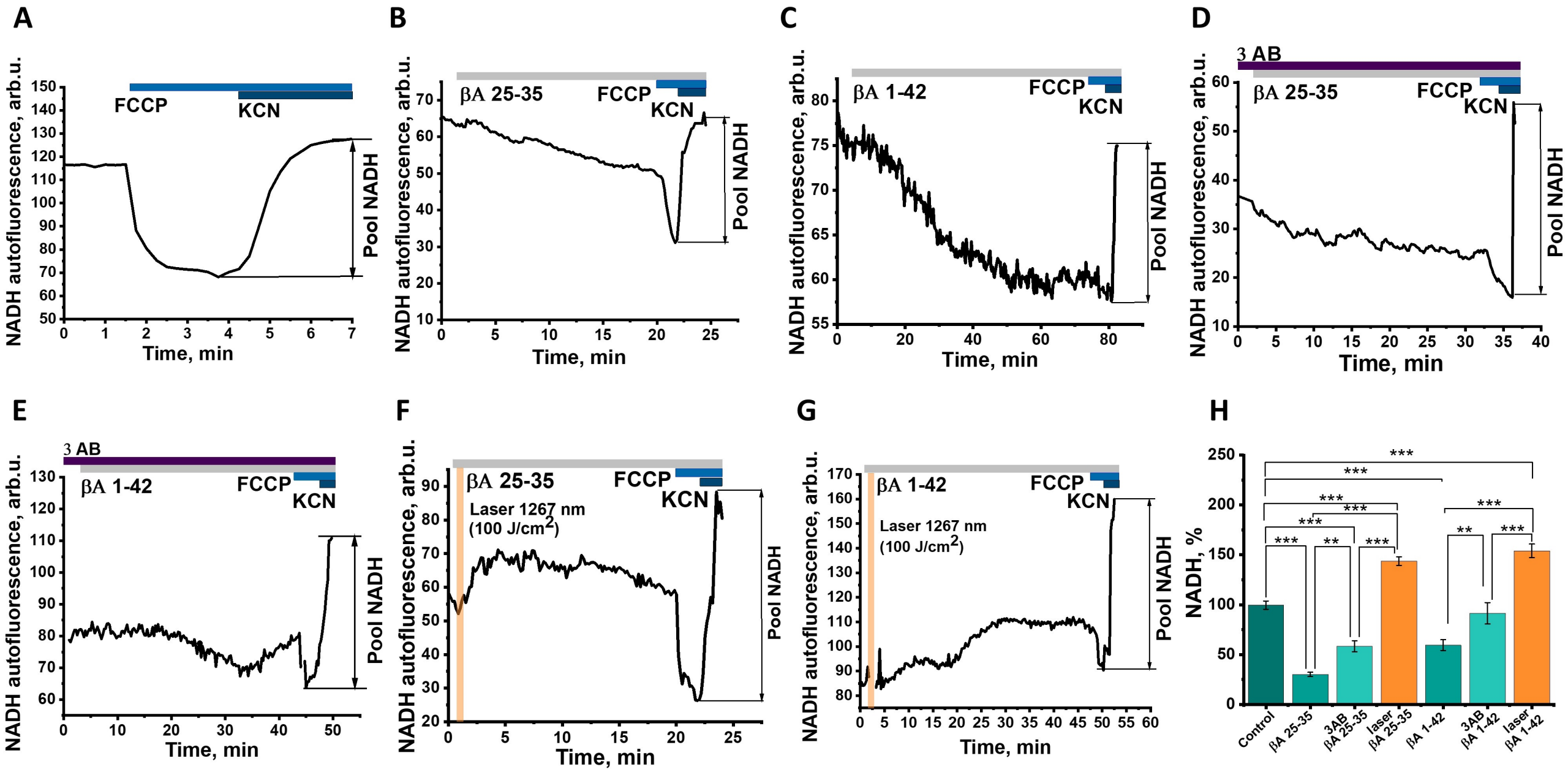
A
B
C
D
E
F
G
H
NADH autofluorescence, arb.u.
Time, min
FCCP
KCN
Pool NADH
βA 25-35
βA 1-42
3 AB
Laser 1267 nm
(100 J/cm2)
NADH, %
Control
βA 25-35
3AB βA 25-35
laser βA 25-35
βA 1-42
3AB βA 1-42
laser βA 1-42
***
**

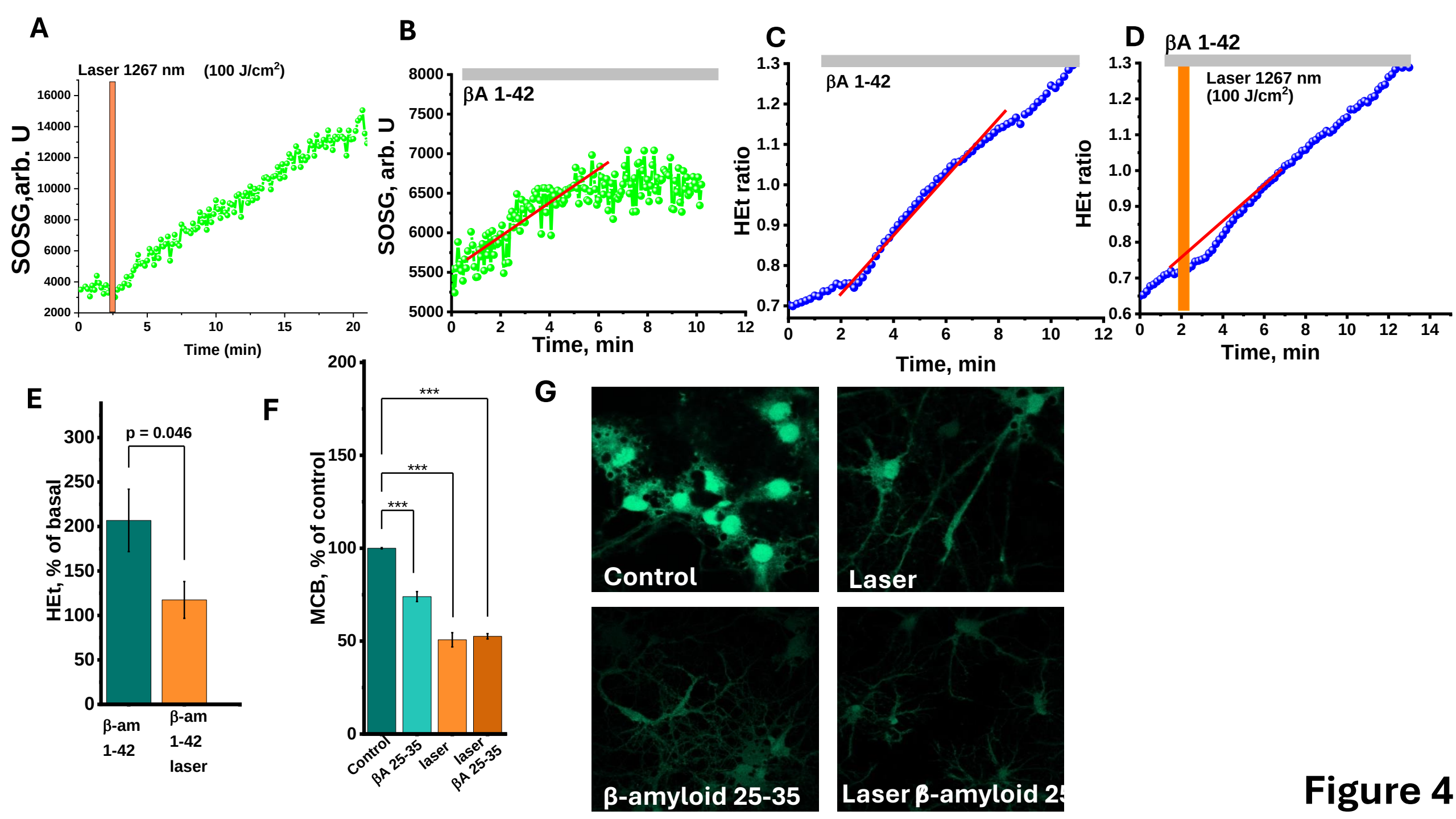
A
Laser 1267 nm (100 J/cm²)
SOSG,arb. U
Time (min)
B
βA 1-42
SOSG, arb. U
Time, min
C
βA 1-42
HEt ratio
Time, min
D
βA 1-42
Laser 1267 nm
(100 J/cm²)
HEt ratio
Time, min
E
p = 0.046
HEt, % of basal
β-am 1-42
β-am 1-42 laser
F
MCB, % of control
***
***
***
Control
βA 25-35
laser
laser βA 25-35
G
Control
Laser
β-amyloid 25-35
Laser β-amyloid 25

Figure 4

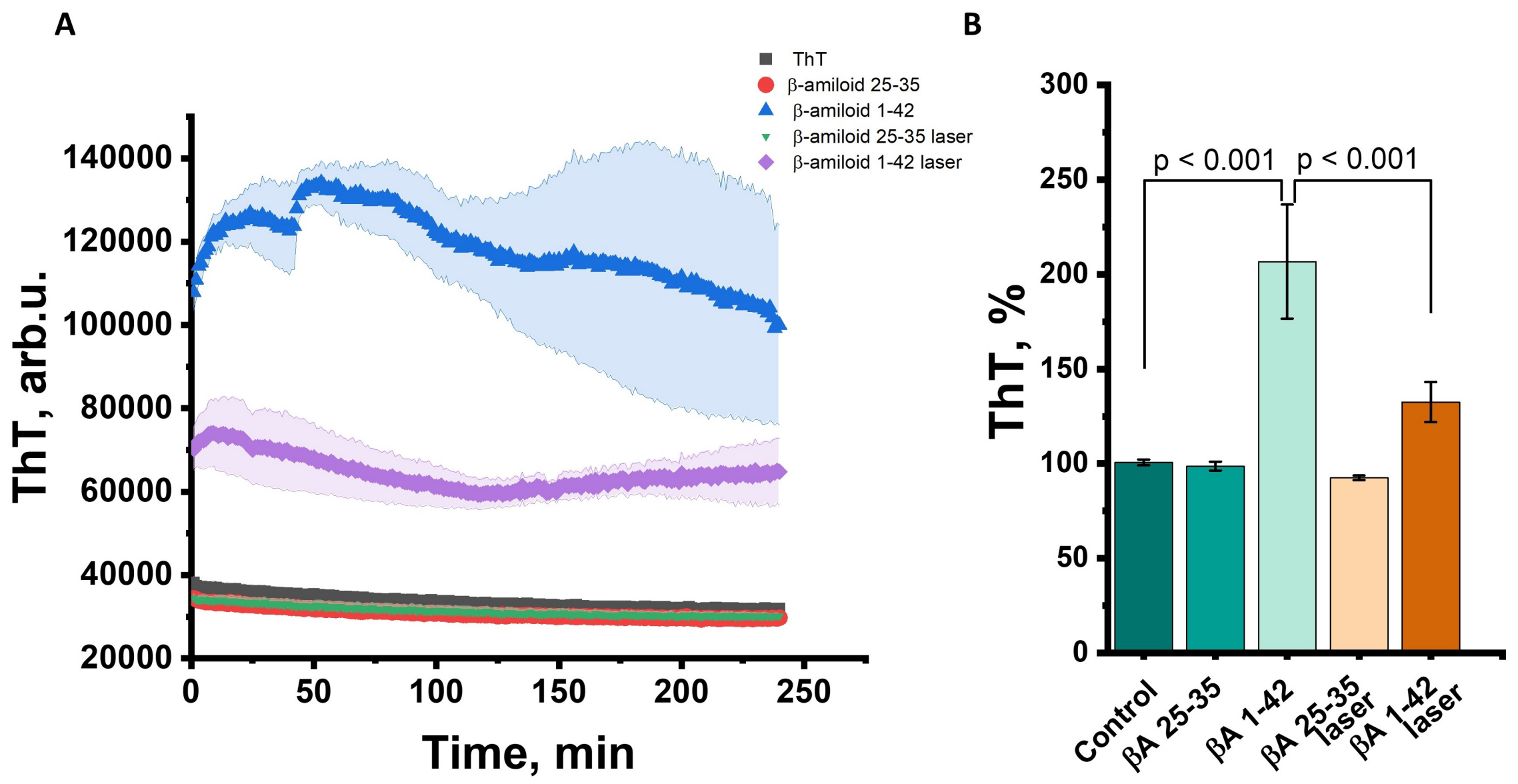
A
ThT
β-amiloid 25-35
β-amiloid 1-42
β-amiloid 25-35 laser
β-amiloid 1-42 laser
ThT, arb.u.
140000
120000
100000
80000
60000
40000
20000
0
50
100
150
200
250
Time, min
B
ThT, %
300
250
200
150
100
50
0
p < 0.001
p < 0.001
Control
βA 25-35
βA 1-42
βA 25-35 laser
βA 1-42 laser

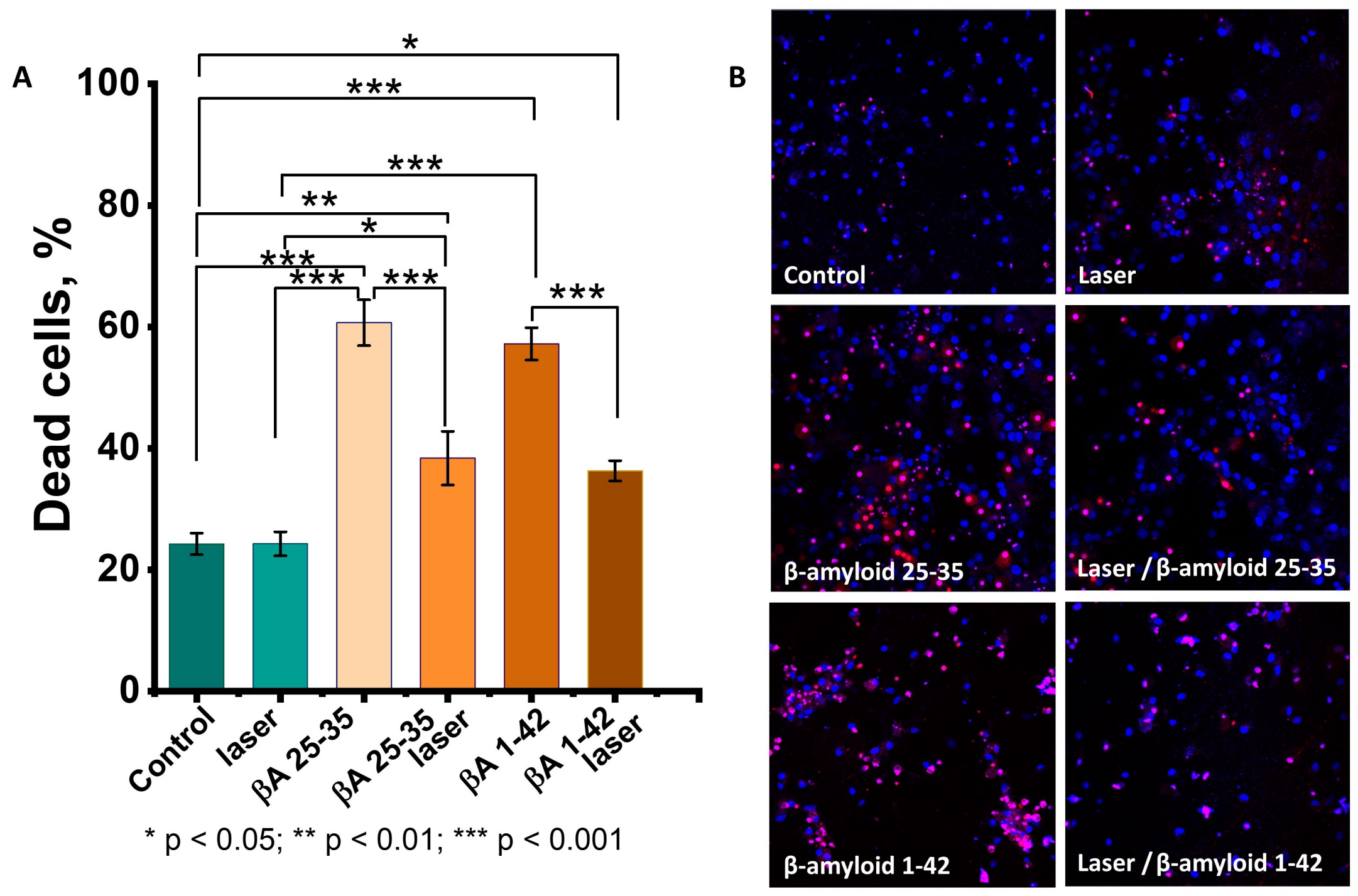
A
B
Dead cells, %
100
80
60
40
20
0
*
***
***
**
*
***
***
***
***
Control
laser
βA 25-35
βA 25-35 laser
βA 1-42
βA 1-42 laser
* p < 0.05; ** p < 0.01; *** p < 0.001
Control
Laser
β-amyloid 25-35
Laser / β-amyloid 25-35
β-amyloid 1-42
Laser / β-amyloid 1-42